THE ASTROPHYSICAL JOURNAL, 369: 169–174, 1991 March 1

FOSSIL DCN IN ORION-KL

JEFFREY G. MANGUM[1,2]
National Radio Astronomy Observatory;[3] and University of Virginia
RICHARD L. PLAMBECK
Radio Astronomy Laboratory, University of California, Berkeley, CA 94720
AND
ALWYN WOOTTEN
National Radio Astronomy Observatory,[3] Edgemont Road, Charlottesville, VA 22903
Received 1990 July 13; accepted 1990 August 21

ABSTRACT

The $J = 1 \rightarrow 0$ transition of DCN was mapped toward Orion-KL with the BIMA array. With a synthesized beam width of 7".6, we identify emission from the "hot core," "compact ridge," and "northern cloud" regions. Over half of the integrated DCN emission detected originates from the hot core component, with progressively smaller contributions from the compact ridge and northern cloud. The DCN fractional abundance is 10^{-9} in the hot core, 4×10^{-10} in the compact ridge, and 2×10^{-10} in the northern cloud; we estimate that the corresponding [DCN]/[HCN] ratios are ~0.005, 0.02, and 0.02. Chemical models suggest that such high [DCN]/[HCN] abundance ratios are produced only in clouds colder than ~20 K. Since the present temperatures near Orion-KL are 50–275 K, it is evident that most of the DCN formed *before* this region was heated by massive star formation. Much of the fossil DCN which we now observe may have sublimated from icy grain mantles.

Subject headings: interstellar: abundances — interstellar: molecules — nebulae: Orion nebula — deuterium

1. INTRODUCTION

The study of deuterium in the interstellar medium has implications for many astrophysical problems. In astrochemistry, measurements of the deuteration in interstellar molecules can provide information on the physical environment and the chemical and dynamical history of a molecular cloud. Because of the zero-point energy difference between hydrogen and deuterium, deuterium-bearing molecules become heavily fractionated in cooler environments (Watson 1976; Dalgarno & Lepp 1984; Wootten 1987). This fractionation can cause the abundances of deuterated molecular species to rise by as much as three orders of magnitude, making them easy to detect.

The abundances of deuterated molecules observed toward the Orion-KL star-forming region present a problem for the interstellar chemist. Even though Orion-KL is a warm ($T_K \simeq$ 50–275 K) region, where deuterium fractionation should not be strongly favored, the observed deuterium enrichments can be as high as those found in cold clouds. Sublimation of icy grain mantles provides a possible explanation for this discrepancy (Walmsley et al. 1987; Plambeck & Wright 1987; Henkel et al. 1987; Mauersberger et al. 1988): perhaps the deuterated species formed at an earlier time when the cloud was much colder, and have been liberated from grain mantles only within the last $\sim 10^4$ yr, as newly formed stars have heated the molecular cloud.

The Orion-KL region consists of several chemically distinct subsources which may have quite different deuterium fractionation. Aperture synthesis maps of the 1_{10}–1_{11} transition of deuterated water (Plambeck & Wright 1987) showed that HDO was abundant in the "hot core" and "compact ridge" subsources, which are the warmest zones near the star IRc 2. HDO emission was not detected toward the cooler ($T_K \simeq 50$ K) "northern cloud," but this could be an excitation effect, since the 1_{10} HDO energy level lies 47 K above the ground state. HDO measurements are not ideal for determining deuterium fractionation because the abundance of nondeuterated water is poorly known.

In this paper we present 7".6 resolution maps of the $J = 1 \rightarrow 0$ transition of DCN toward Orion-KL. The DCN data provide a good probe of the deuterium fractionation in all of the Orion subsources because the $J = 1$ energy level lies only 3.5 K above the ground state, and because the corresponding HCN column densities can be determined from observations of the less abundant isotopic species $H^{13}CN$ and $HC^{15}N$.

2. OBSERVATIONS

Data were obtained using 8 configurations of the three-element BIMA array[4] at the Hat Creek Radio Observatory between 1988 December and 1989 October. Projected antenna spacings ranged from 1.4 kλ to 29 kλ. At 72 GHz, the three 6.1 m diameter antennas have primary beam widths of ~2'.7. The phase tracking center was $\alpha(1950) = 05^h32^m47^s.0$, $\delta(1950) = -05°24'21''$, ~3" north of IRc 2. The quasars 0420−014 and 0528+134 were used as phase calibrators. Observations of 3C 273 were used to calibrate the instrumental passband each day. The amplitude scale was referenced to 0420−014; its 72 GHz flux density, measured from time to time by comparison with

[1] National Radio Astronomy Observatory Junior Research Associate.

[2] Postal address: Astronomy Department, University of Texas, Austin, TX 78712.

[3] The National Radio Astronomy Observatory is operated by Associated Universities, Inc., under cooperative agreement with the National Science Foundation.

[4] Operated by the University of California at Berkeley, the University of Illinois, and the University of Maryland, with support from the National Science Foundation.

TABLE 1

DCN $J = 1 \rightarrow 0$ REST FREQUENCIES[a]

Transition[b]	Frequency (GHz)	Relative Intensity[c]
$F_N = 1 \rightarrow 1, F_D = 1 \rightarrow 0, 1, 2$	72.413484	...
$F_N = 1 \rightarrow 1, F_D = 2 \rightarrow 1, 2$	72.413514	0.33
$F_N = 1 \rightarrow 1, F_D = 0 \rightarrow 0, 1$	72.413558	...
$F_N = 2 \rightarrow 1, F_D = 1 \rightarrow 0, 1, 2$	72.414905	...
$F_N = 2 \rightarrow 1, F_D = 3 \rightarrow 2$	72.414927	0.56
$F_N = 2 \rightarrow 1, F_D = 2 \rightarrow 1, 2$	72.414973	...
$F_N = 0 \rightarrow 1, F_D = 1 \rightarrow 0, 1, 2$	72.417030	0.11

[a] From DeLucia & Gordy 1969.

[b] Each transition is designated by a nitrogen quadrupole quantum number (F_N) and a deuterium magnetic dipole quantum number (F_D).

[c] Only the relative intensities of the strongest hyperfine components are given.

planets, was 4.8 ± 0.3 Jy over the course of the observations. The uncertainty in the absolute flux calibration is estimated to be ±15%. With the receivers tuned to their low-frequency limit, the single sideband system temperatures were 500–900 K, scaled to outside the atmosphere.

The DCN rest frequencies are given in Table 1. The $J = 1 \rightarrow 0$ transition consists of three well-separated hyperfine components; additional splittings within the $F_N = 1 \rightarrow 1$ and $F_N = 2 \rightarrow 1$ components are less than 0.07 MHz, or 0.3 km s^{-1}, smaller than the line widths in Orion-KL. Spectra were obtained with a digital cross-correlation spectrometer, configured to give a velocity resolution of 0.32 km s^{-1} over an 80 km s^{-1} wide velocity range. To increase signal-to-noise, the data were smoothed to a velocity resolution of 0.65 km s^{-1}.

The data were mapped and CLEANed using the RALINT data reduction package developed at U.C. Berkeley. The synthesized beam width was 7''.9 × 7''.4 and the RMS noise was 0.625 Jy beam^{-1} (2.5 K) in individual 0.65 km s^{-1} wide velocity channels.

3. RESULTS

On arcminute scales, Orion-KL is composed of a ridge of dense gas running northeast-southwest. Closer inspection of this ridge reveals the presence of several emission components which are distinguishable through their spatial, dynamical, and chemical signatures (see Blake et al. 1987). We find that three of these components, the "hot core," "compact ridge," and "northern cloud" (sometimes called the "10 km s^{-1} feature"), are strong sources of DCN emission.

3.1. *Hot Core*

In Figure 1 we show the total integrated $J = 1 \rightarrow 0$ DCN emission over a 24 km s^{-1} velocity interval from the uniformly weighted maps. Approximately 60% of the integrated emission originates from the ~8'' diameter clump centered ~4'' southwest of IRc 2. The central velocity ($V_{LSR} \simeq 6$ km s^{-1}) and velocity width (FWHM $\simeq 6$ km s^{-1}) of the DCN spectrum toward this condensation identifies it as the hot core spectral feature. The peak brightness temperature from this source is 10 K in a 7''.9 × 7''.4 beam.

3.2. *Compact Ridge*

It is difficult to identify the compact ridge and northern cloud emission components in Figure 1 because the integrated intensity map is dominated by broad velocity emission from

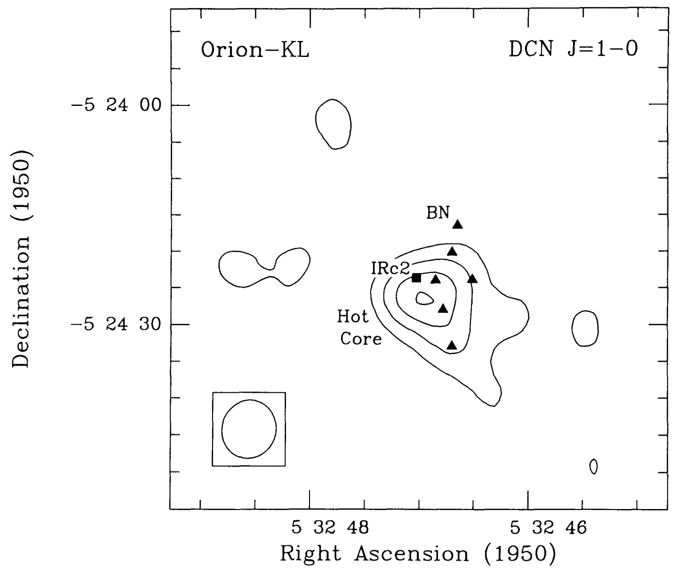

FIG. 1.—Integrated intensity map of the $J = 1 \rightarrow 0$ transition of DCN toward Orion-KL. The velocity interval for the integration was 24 km s^{-1} and the contours are 48, 72, 96, and 120 K km s^{-1}; offsets due to dust continuum emission (see § 4.1) have not been subtracted. The 1 σ noise level in this map is 12 K km s^{-1}. Positions of the 20 μm sources IRc 1–7 (Downes et al. 1981) are indicated; IRc 2 is denoted by a filled box, the other sources by filled triangles; BN = IRc 1. The 7''.9 × 7''.4 synthesized beam is shown in the lower left corner. DCN emission peaks toward the hot core, just south of IRc 2.

the hot core. Since the compact ridge spectral feature has a fairly well-determined LSR velocity of 8 km s^{-1} and a FWHM velocity width of 3 km s^{-1}, we show in Figure 2 a map of the strongest DCN hyperfine component ($F_N = 2 \rightarrow 1$) over this velocity range. The emission region centered near IRc 5 is the compact ridge. The DCN map in Figure 2 closely resembles high-resolution maps of H_2CO (Mangum et al. 1990) and CH_3OH (Plambeck & Wright 1988b) compact ridge emission.

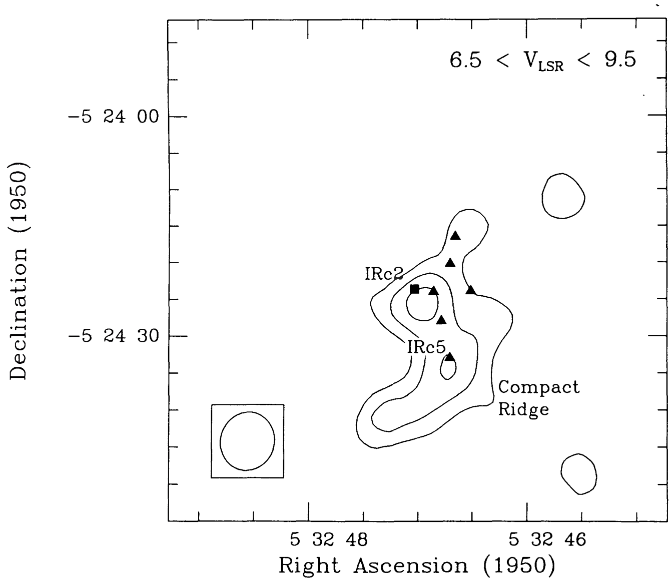

FIG. 2.—Map of the $J = 1 \rightarrow 0$, $F_N = 2 \rightarrow 1$ transition of DCN integrated over a 3 km s^{-1} velocity range centered at $V_{LSR} = 8$ km s^{-1}. Contours are 10.8, 16.2, and 21.6 K km s^{-1}. The 1 σ noise level in this map is 3.5 K km s^{-1}. The synthesized beam and positions of IRc 1–7 are shown as in Fig. 1. Emission from the compact ridge, centered approximately on IRc 5, is prominent.

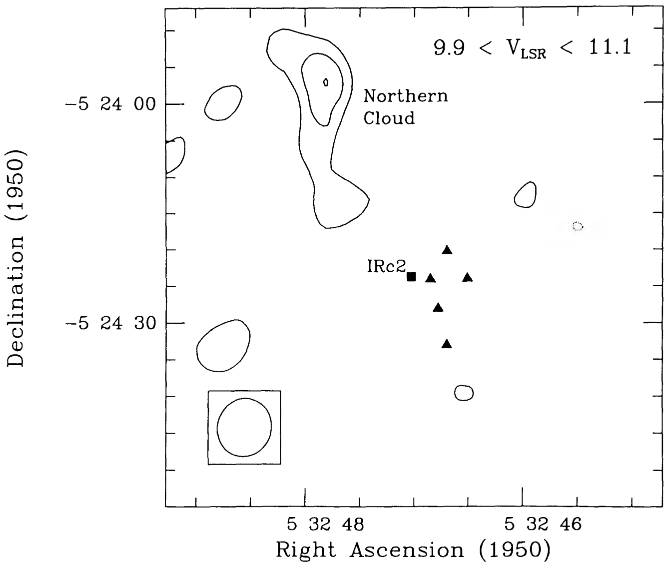

FIG. 3.—Map of the $J = 1 \rightarrow 0$, $F_N = 2 \rightarrow 1$ transition of DCN integrated over a 1.2 km s^{-1} velocity range centered at $V_{LSR} = 10.5$ km s^{-1}. Contours are 6, 9, and 12 K km s^{-1}. The 1 σ noise level in this map is 2 K km s^{-1}. The synthesized beam and positions of IRc 1–7 are shown as in Fig. 1. Emission in this narrow velocity interval is dominated by the northern cloud.

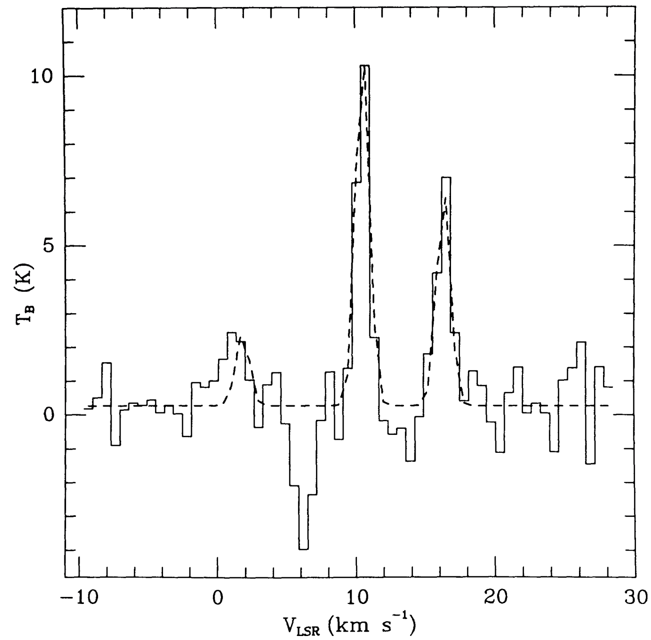

FIG. 4.—$J = 1 \rightarrow 0$ DCN spectrum of the northern cloud, generated from maps convolved to 12″ × 8″ resolution. The intensity ratio of the hyperfine components is 5:3:1, consistent with optically thin emission.

The peak DCN brightness temperature toward IRc 5 is ~8 K in our 7″.9 × 7″.4 beam.

3.3. *Northern Cloud*

The northern cloud (sometimes referred to as the "10 km s^{-1} feature") is a condensation within the Orion "ridge" located ~25″ northeast of IRc 2; it corresponds to continuum source CS1 of Mundy et al. (1986). Emission from the northern cloud is prominent in $V_{LSR} = 10.5$ km s^{-1} maps of CS, HC_3N, HCN, CH_3CN, and H_2CO (Mundy et al. 1988; Masson & Mundy 1988; Plambeck & Wright 1988a; Mangum et al. 1990). The gas within the northern cloud is relatively quiescent; line widths are typically 1–1.5 km s^{-1} (FWHM).

Figure 3 presents a map of the strongest DCN hyperfine component over the velocity range 9.9–11.1 km s^{-1}. The peak brightness temperature is 10 K. A spectrum through the peak position is shown in Figure 4. Because the line widths are so narrow, we can easily resolve the three main hyperfine components; their amplitudes are in the ratio 5:3:1, consistent with optically thin emission.

4. ABUNDANCE ESTIMATES

4.1. *Continuum Subtraction*

Table 2 lists the DCN integrated intensities toward the hot core, compact ridge, and northern cloud peak positions. These are the intensities in our 7″.9 × 7″.4 beam, summed over the three principal DCN hyperfine components, and corrected for offsets due to dust continuum emission. The continuum corrections are based on the 95 GHz maps of Mundy et al. (1986), which show that the fluxes toward the hot core, compact ridge, and northern cloud are 0.95, ~0.5, and 0.36 Jy beam^{-1}, respectively, in a 7″.5 beam. Wright & Vogel (1985) found that the millimeter-wavelength dust opacity varies as $\nu^{1.3}$. Therefore, after converting to brightness temperature, we estimate that continuum emission at 72.4 GHz contributes 1.6, 0.8, and 0.6 K to the hot core, compact ridge, and northern cloud maps. The dust continuum correction significantly affects only the hot core integrated intensity.

4.2. *Column Densities*

In order to estimate the fractional abundance of DCN, we first need to calculate N_{tot} (DCN), the total DCN column

TABLE 2

DCN FRACTIONAL ABUNDANCE ESTIMATES

Component	α(1950)	δ(1950)	$\int T_B dv$[a] (K km s^{-1})	FWZI (km s^{-1})	T_K[b] (K)	N_{tot} (DCN) (10^{14} cm^{-2})	N (H_2)[c] (10^{24} cm^{-2})	X (DCN) (10^{-10})
Hot core	05ʰ32ᵐ46ˢ.9	−05°24′26″	67	~10	200	19.9	2.0	10.0
Compact ridge	05 32 46.7	−05 24 33	25	3.2	100	3.8	1.0	3.8
Northern cloud	05 32 47.8	−05 23 59	22	1.5	50	1.7	1.0	1.7

[a] 37.3, 7.8, and 2.4 K km s^{-1} have been subtracted from the hot core, compact ridge, and northern cloud measured integrated intensities, respectively, to compensate for the contribution to the emission due to dust continuum toward these components.

[b] The kinetic temperature measurements are from the following references: hot core, Blake et al. 1987; compact ridge, Loren & Mundy 1984; northern cloud, Plambeck & Wright 1988a.

[c] From 95 GHz dust continuum measurements (Mundy et al. 1986).

density, toward each Orion-KL component. Assuming that the DCN rotational energy levels are in local thermodynamic equilibrium (LTE) and that $T_{ex} \gg T_{bg}$, the total DCN column density from the $J = J_u \rightarrow J_l$ transition is given by

$$N_{tot}(\mathrm{DCN}) = \frac{3hQ_{rot}}{8\pi^3 |\mu_{J_l J_u}|^2} \left[\exp\left(\frac{h\nu}{kT_{ex}}\right) - 1\right]^{-1} \times \exp\left(\frac{E_u}{T_{ex}}\right) \int \tau\, dV \ \mathrm{cm}^{-2} ,$$

where $|\mu_{J_l J_u}|^2$ is the molecular dipole moment matrix element, Q_{rot} is the rotational partition function, and the other symbols have their usual meanings. For DCN, $|\mu_{J_l J_u}|^2 = \mu^2_{J_u}$ and $\mu = 2.985$ Debye [Maki 1974; assuming that $\mu(\mathrm{DCN}) = \mu(\mathrm{HCN})$]. Assuming that $h\nu \ll kT_{ex}$, the rotational partition function is $Q_{rot} \simeq kT_{ex}/hB_0$. Therefore, for the $J = 1 \rightarrow 0$ transition, where $B_0 = 36.2075$ GHz (DeLucia & Gordy 1969) and $E_u = 3.48$ K, the equation for the column density becomes

$$N_{tot}(\mathrm{DCN}) = \frac{3k^2 T_K T_{ex}}{8\pi^3 h B_0 \mu^2 J_u \nu} \exp\left(\frac{E_u}{T_{ex}}\right) \int \tau\, dV \ \mathrm{cm}^{-2} ,$$

which, for $\tau \ll 1$ and $T_{ex} = T_K$, becomes

$$N_{tot}(\mathrm{DCN}) = 1.47 \times 10^{11} T_K \exp\left(\frac{3.48}{T_K}\right) \int T_B\, dV \ \mathrm{cm}^{-2} ,$$

where dV is the velocity width in km s^{-1}. Table 2 gives the results of this calculation using the measured peak integrated intensities and kinetic temperatures listed.

To confirm that the LTE column densities in Table 2 were reasonable, we also performed statistical equilibrium calculations using the HCN collisional rates given by Green & Thaddeus (1974); for molecular hydrogen densities greater than 10^5 cm^{-3}, DCN column densities derived from the non–LTE calculation differ by less than a factor of 3 from those in Table 2.

4.3. *Fractional Abundances*

The last column in Table 2 lists the fractional abundances, $X(\mathrm{DCN}) = [N_{tot}(\mathrm{DCN})]/[N(\mathrm{H_2})]$, calculated from our column density measurements and from the H_2 column densities derived by Mundy et al. (1986), which are inferred from dust continuum observations. The DCN fractional abundance appears to be highest toward the hot core, the warmest of the Orion-KL components.

DCN column densities must be compared with HCN column densities in order to determine the level of deuterium fractionation in each of the Orion-KL components. Although Vogel et al. (1985) made 6″ resolution observations of the $J = 1 \rightarrow 0$ HCN transition toward Orion-KL which show the hot core, compact ridge, and northern cloud components quite prominently, this transition is likely to be optically thick, making it a poor tracer of HCN column density. Accordingly, we base our HCN column density estimates on single antenna observations of the less abundant isotopic species $H^{13}CN$ and $HC^{15}N$, reported by Blake et al. (1987) and by Rydbeck et al. (1981). These observations identify contributions from the various Orion subsources by deconvolving their characteristic spectral components from the line profiles.

Blake et al. (1987) tabulate the HCN column density toward the hot core and "extended ridge." Since the northern cloud lies outside the 30″ beam used by Blake et al., we assume that the "ridge" emission originates primarily in the compact ridge. From our DCN maps in Figures 1–3 we estimate that the hot core, compact ridge, and northern cloud have effective source diameters of ~8″, ~15″, and ~15″, respectively. The column densities reported by Blake et al. are averaged over a 30″ beam; dividing them by the hot core and compact ridge beam filling factors, and scaling the "ridge" value upward by another factor of 5 to correct for the difference in rotational temperatures assumed (Blake et al. use 20 K; we use 100 K), we infer $N_{tot}(\mathrm{HCN}) \simeq 4 \times 10^{17}$ cm^{-2} for the hot core and 2×10^{16} cm^{-2} for the compact ridge.

Rydbeck et al. (1981) were able to detect only a weak hot core feature in $H^{13}CN$ and $HC^{15}N$ spectra taken with a 43″ beam but identify emission from both "ridge I" ($V_{LSR} \simeq 8$ km s^{-1}) and "ridge II" ($V_{LSR} \simeq 10$ km s^{-1}) components, which we identify with the compact ridge and the northern cloud. Scaling up their $H^{13}CN$ column densities by an assumed [HCN]/[$H^{13}CN$] abundance ratio of 40 (see Blake et al. 1987), correcting to our assumed excitation temperatures, and dividing by the appropriate beam filling factors, we infer $N_{tot}(\mathrm{HCN}) \simeq 2 \times 10^{16}$ cm^{-2} for the compact ridge (in agreement with the value derived from the data of Blake et al.) and $N_{tot}(\mathrm{HCN}) \simeq 8 \times 10^{15}$ cm^{-2} for the northern cloud.

These estimates imply that [DCN]/[HCN] $\simeq 0.005$ in the hot core and 0.02 in the compact ridge and northern cloud. Owing to the large number of assumptions needed to derive the HCN column densities, these values are uncertain by at least a factor of two; aperture synthesis maps of $H^{13}CN$ and $HC^{15}N$ are needed in order to determine the fractionation more accurately.

5. DISCUSSION

The [DCN]/[HCN] ratios we find toward Orion-KL are about a factor of 1000 greater than the cosmic D/H ratio of $\sim 10^{-5}$. The compact ridge and northern cloud ratios are comparable with the ratio [DCN]/[HCN] $= 0.023 \pm 0.01$ found in the dark cloud TMC-1 (Wootten 1987).

Such large deuterium enrichments cannot be explained with gas-phase chemistry, if this chemistry takes place at the temperatures presently characteristic of Orion-KL. Millar, Bennett, & Herbst (1989) have modeled the deuterium fractionation in dense interstellar clouds using a pseudo–time-dependent gas-phase chemical model. In their "early time" models, Millar, Bennett, and Herbst predict that [DCN]/[HCN] $= 0.0035$ at $T_K = 70$ K and that [DCN]/[HCN] should slowly *increase* with increasing temperature. This slow increase in [DCN]/[HCN] is due completely to the neutral-neutral reaction

$$\mathrm{N + CHD \rightarrow DCN + H}$$

whose reaction rate has not been measured but is estimated by Millar, Bennett, and Herbst to have an activation energy of ~50 K. There is also considerable uncertainty regarding the dissociative recombination branching ratios used in these chemical models. Using alternative branching ratios based on the ideas of Bates (1986, 1987), Millar, Bennett, and Herbst predict that at "early times" [DCN]/[HCN] $= 0.012$ at $T_K = 70$ K and that [DCN]/[HCN] should slowly *decrease* with increasing temperature. Given these uncertainties, we will assume that [DCN]/[HCN] $\simeq 0.001$ in the range $50 \leq T_K \leq 200$ K. Our measurements indicate that the [DCN]/[HCN] ratios in the Orion-KL region are roughly an order of magnitude greater than the gas-phase chemical models predict.

In order to make up for the shortcomings of the gas-phase chemical models, icy grain mantles have been proposed as a possible source of the excess in deuterated molecules (Walmsley et al. 1987; Plambeck & Wright 1987; Henkel et al. 1987; Tielens & Allamandola 1987a, b; Mauersberger et al. 1988; Turner 1990). By depositing high concentrations of deuterium-bearing compounds onto icy grain surfaces during the early, low-temperature phase of molecular cloud evolution, one can build a reservoir of deuterated species. Some heating event, like the formation of a nearby star, can then release this fossil deuterium from the grain mantles into the gas phase. Again referring to the "early time" gas-phase chemical models of Millar, Bennett, & Herbst (1989), our measured [DCN]/[HCN] ratio of 0.005 for the hot core would imply that the chemistry occurred at a temperature of 25 K. For the compact ridge and northern cloud components, where the observed [DCN]/[HCN] ratio is 0.02, the gas-phase chemistry must have occurred when $T_K \lesssim 10$ K.

In a similar chemical calculation, but which included the influence of dust grains, Brown, Charnley, & Millar (1988) and Brown & Millar (1989) have developed a detailed time-dependent chemical model to describe the chemical composition of hot molecular cores in dense star-forming regions like Orion-KL. By following the chemical evolution of a cold collapsing molecular cloud, including the accretion and subsequent reaction of material on the surfaces of grains, they make predictions of the molecular abundances in hot core sources. Brown & Millar (1989) predict $X(\mathrm{DCN}) = 1.1 \times 10^{-8}$ and [DCN]/[HCN] = 0.02. The predicted DCN abundance is ~ 10, 25, and 50 times our observed hot core, compact ridge, and northern cloud DCN abundances. The predicted [DCN]/[HCN] ratio is ~ 4 times larger than our calculated hot core ratio and approximately equal to the compact ridge and northern cloud ratios. The observed agreement between this model and the observations, though, might be fortuitous because Brown and Millar omitted H abstraction and addition reactions whose activation barriers differ between H and D isotopic species, and which may produce a much greater deuterium enhancement if omitted. Furthermore, since the reaction which would form HCN and DCN on a grain surface involves CH_2 and N, both of which will have low abundances, the X(DCN) and [DCN]/[HCN] predicted by the model must reflect the initial conditions assumed in the model calculation. Brown and Millar assumed an initial cloud temperature of 10 K, which would have much more HCN deuterium fractionation than a cloud at 25 K. Therefore, the fact that Brown and Millar overpredict [DCN]/[HCN] in the hot core is probably due to their use of a low initial temperature for this component.

The chemical models suggest that most of the DCN we presently observe toward Orion-KL formed at an earlier time when the cloud was much colder. Downes et al. (1981) estimate that the outflow from IRc 2 is 10^3–10^4 yr old; it is likely that the molecular gas near IRc 2 has been heated to its present temperatures during this short time. Walmsley et al. (1987) and Brown, Charnley, & Millar (1988) argue that more than 10^4 yr are required to approach chemical equilibrium in the hot core, owing to the low abundance of molecular ions in such a dense region. Therefore, it is not surprising that the [DCN]/[HCN] ratio observed toward the hot core is characteristic of a much colder region.

Much of the DCN toward the hot core and compact ridge may have sublimated from grain mantles, although our observations, and theoretical estimates of the molecular composition of grain mantles do not require this. Certainly very little of the observed DCN formed on grain surfaces. D'Hendecourt, Allamandola, & Greenberg (1985) have studied the time-dependent chemistry of grain surface reactions and find that radical reactions of the kind which produce HCN and DCN on the surfaces of grains are negligible. Also, one may question how sublimation from grain mantles could be a substantial contributor to the northern cloud DCN abundance since this region is colder than the 65–90 K condensation temperatures which Nakagawa (1980) calculates for molecules such as HCN and H_2O.

6. CONCLUSIONS

The Orion-KL hot core, compact ridge, and northern cloud have been observed to be strong emitters of $J = 1 \rightarrow 0$ DCN emission. More than half of the DCN emission originates from the hot core component, which is the warmest source in the region. The [DCN]/[HCN] ratio is estimated to be $\simeq 0.005$ in the hot core and 0.02 in the compact ridge and the northern cloud. According to chemical models, such high [DCN]/[HCN] ratios are produced only in clouds colder than ~ 25 K, whereas the present temperatures in the Orion-KL region range from 50 to 275 K. Presumably most of the DCN in Orion-KL was produced before massive star formation heated the cloud. Toward the hot core and compact ridge, much of the DCN may have been released from icy grain mantles, although neither current theory nor our observations *require* the use of grain mantles as a repository of fossil DCN.

J. G. M. would like to thank the National Radio Astronomy Observatory for support through a Junior Research Associateship. The BIMA observations were supported in part by NSF Grant AST 87-14721.

REFERENCES

Bates, D. R. 1986, ApJ, 306, L45

———. 1987, in Modern Applications of Atomic and Molecular Physics, ed. A. E. Kingston (London: Plenum), p. 41

Blake, G. A., Sutton, E. C., Masson, C. R., & Phillips, T. G. 1987, ApJ, 315, 621

Brown, P. D., Charnley, S. B., & Millar, T. J. 1988, MNRAS, 231, 409

Brown, P. D., & Millar, T. J. 1989, MNRAS, 237, 661

Dalgarno, A., & Lepp, S. 1984, ApJ, 287, L47

DeLucia, F., & Gordy, W. 1969, PhyRv, 187, 58

d'Hendecourt, L. B., Allamandola, L. J., & Greenberg, J. M. 1985, A&A, 152, 130

Downes, D., Genzel, R., Becklin, E. E., & Wynn-Williams, C. G. 1981, ApJ, 244, 869

Green, S., & Thaddeus, P. 1974, ApJ, 191, 653

Henkel, C., Mauersberger, R., Wilson, T. L., Snyder, L. E., Menten, K. M., & Wouterloot, J. G. A. 1987, A&A, 182, 299

Loren, R. B., & Mundy, L. G. 1984, ApJ, 286, 232

Maki, A. G. 1974, JPCRD, 3, 221

Mangum, J. G., Wootten, A., Loren, R. B., & Wadiak, E. J. 1990, ApJ, 348, 542

Masson, C. R., & Mundy, L. G. 1988, ApJ, 324, 538

Mauersberger, R., Henkel, C., Jacq, T., & Walmsley, C. M. 1988, A&A, 194, L1

Millar, T. J., Bennett, A., & Herbst, E. 1989, ApJ, 340, 906

Mundy, L. G., Cornwell, T. J., Masson, C. R., Scoville, N. Z., Bååth, L. B., & Johansson, L. E. B. 1988, ApJ, 325, 382

Mundy, L. G., Scoville, N. Z., Bååth, L. B., Masson, C. R., & Woody, D. P. 1986, ApJ, 304, L51

Nakagawa, N. 1980, in IAU Symposium 87, Interstellar Molecules, ed. B. H. Andrew (Dordrecht: Reidel), p. 365

Plambeck, R. L., & Wright, M. C. H. 1987, ApJ, 317, L101

———. 1988a, in Molecular Clouds in the Milky Way and External Galaxies, ed. R. L. Dickman, R. L. Snell, & J. S. Young (New York: Springer-Verlag), p. 182

———. 1988b, ApJ, 330, L61

Rydbeck, O. E. H., Hjalmarson, Å, Rydbeck, G., Elldér, J., Olofsson, H., & Sume, A. 1981, A&A, 243, L41
Tielens, A. G. G. M., & Allamandola, L. J. 1987a, in Physical Processes in the Interstellar Medium, ed. G. E. Morfill & M. Scholer (Dordrecht: Reidel), p. 333
———. 1987b, in Interstellar Processes, ed. D. J. Hollenbach & H. A. Thronson, Jr. (Dordrecht: Reidel), p. 397
Turner, B. E. 1990, preprint
Vogel, S. N., Bieging, J. H., Plambeck, R. L., Welch, W. J., & Wright, M. C. H. 1985, ApJ, 296, 600
Walmsley, C. M., Hermsen, W., Henkel, C., Mauersberger, R., & Wilson, T. L. 1987, A&A, 172, 311
Watson, W. D. 1976, RevMoPhys, 48, 513
Wootten, A. 1987, in Astrochemistry, ed. M. S. Vardya & S. P. Tarafdar (Dordrecht: Reidel), p. 311
Wright, M. C. H., & Vogel, S. N. 1985, ApJ, 297, L11